Received: 27 March 2020 | Revised: 12 May 2020 | Accepted: 2 June 2020

DOI: 10.1002/ardp.202000090

FULL PAPER

DPhG ARCH PHARM Archiv der Pharmazie

Synthesis and antidiabetic evaluation of benzimidazole-tethered 1,2,3-triazoles

Laxmi Deswal[1] | Vikas Verma[1] | Devinder Kumar[1] | Chander P. Kaushik[1] | Ashwani Kumar[2] | Yogesh Deswal[1] | Suman Punia[1]

[1]Department of Chemistry, Guru Jambheshwar University of Science and Technology, Hisar, India

[2]Department of Pharmaceutical Sciences, Guru Jambheshwar University of Science and Technology, Hisar, India

Correspondence
Vikas Verma, Department of Chemistry, Guru Jambheshwar University of Science and Technology, Hisar 125001, India.
Email: vikas_chem_pu@yahoo.com

Abstract

Some novel benzimidazole-tethered 1,2,3-triazole derivatives (**4a–r**) were synthesized by a click reaction between 2-substituted 1-(prop-2-yn-1-yl)-1*H*-benzo[*d*]imidazole and in situ azide. The structures of the synthesized compounds were confirmed by spectroscopic studies (one- and two-dimensional nuclear magnetic resonance, Fourier transform infrared, and high-resolution mass spectra). The synthesized compounds were evaluated for their antidiabetic activity. Compounds **4a–r** exhibited a good-to-moderate α-amylase and α-glucosidase inhibitory activity, with IC_{50} values ranging from 0.0410 to 0.0916 μmol/ml and 0.0146 to 0.0732 μmol/ml, respectively. Compounds **4e**, **4g**, and **4n** were found to be most active. Furthermore, the binding conformation of the most active compounds was ascertained by docking studies.

KEYWORDS

1,2,3-triazole, antidiabetic, benzimidazole, docking, α-amylase, α-glucosidase

1 | INTRODUCTION

The International Diabetes Federation in 2019 reported that about 463 million people were suffering from diabetes, and this number is supposed to increase at an alarming rate. It is estimated that 578 million people will have diabetes in 2030 and 700 million in 2045.[1] Type-II diabetes, which is the more common form of the disease (accounts for 95% of the total diabetic population) is characterized by a gradual increase in insulin resistance, followed by the dysfunctioning of pancreatic beta cells, thus leading to hyperglycemia.[2] Diabetes can also lead to other serious health issues such as vision loss, nerve damage, kidney failure, and so forth. One of the important tactics for treating this disease is to control and regulate the blood glucose level by inhibiting carbohydrate hydrolytic enzymes.[3] α-Glucosidase is an important hydrolytic enzyme that plays a key role in digestion of carbohydrates and it converts unabsorbed disaccharides and oligosaccharides into monosaccharides.[4,5] α-Glucosidase inhibitors specifically inhibit α-glucosidase in the brush border of the enterocytes of the jejunum in the small intestine, thus retarding the carbohydrate digestion.[6] Clinically accepted drugs of this class such as acarbose, voglibose, and miglitol are often reported to cause side effects such as abdominal pain, diarrhea, and so forth.[7] Therefore, designing better drugs for the treatment of diabetes has been a challenging area for medicinal chemists.

Benzimidazole can be considered as a privileged structure in medicinal chemistry, and its derivatives exhibit a variety of biological activities including antidiabetic activity.[8–16] Among different triazoles, 1,2,3-triazoles particularly have a broad range of applications in the field of pharmaceutical and medicinal chemistry, and they are a part of many molecules reported as antidiabetic.[17–24] It has been reported that benzimidazole compounds, that is, 2-aryl benzimidazoles (**A**) and 2-(2-chlorophenyl)-7-methyl-1*H*-benzo[*d*]imidazole (**B**), act as α-glucosidase inhibitors,[25–27] but there is still a need to discover some new analogs for improved inhibitory activity. Various studies have reported that by combining a benzimidazole ring with an electron-withdrawing group such as triazole, the biological activity gets enhanced.[28] Compound **C**, a hybrid of 2,4,5-triarylimidazole–triazole, and compound **D**, a hybrid of xanthone–triazole, showed a good antidiabetic activity (Figure 1).[29,30]

Encouraged by the above facts, the synthesis of benzimidazole-tethered 1,2,3-triazoles (**4a–r**), with the objective of discovering new

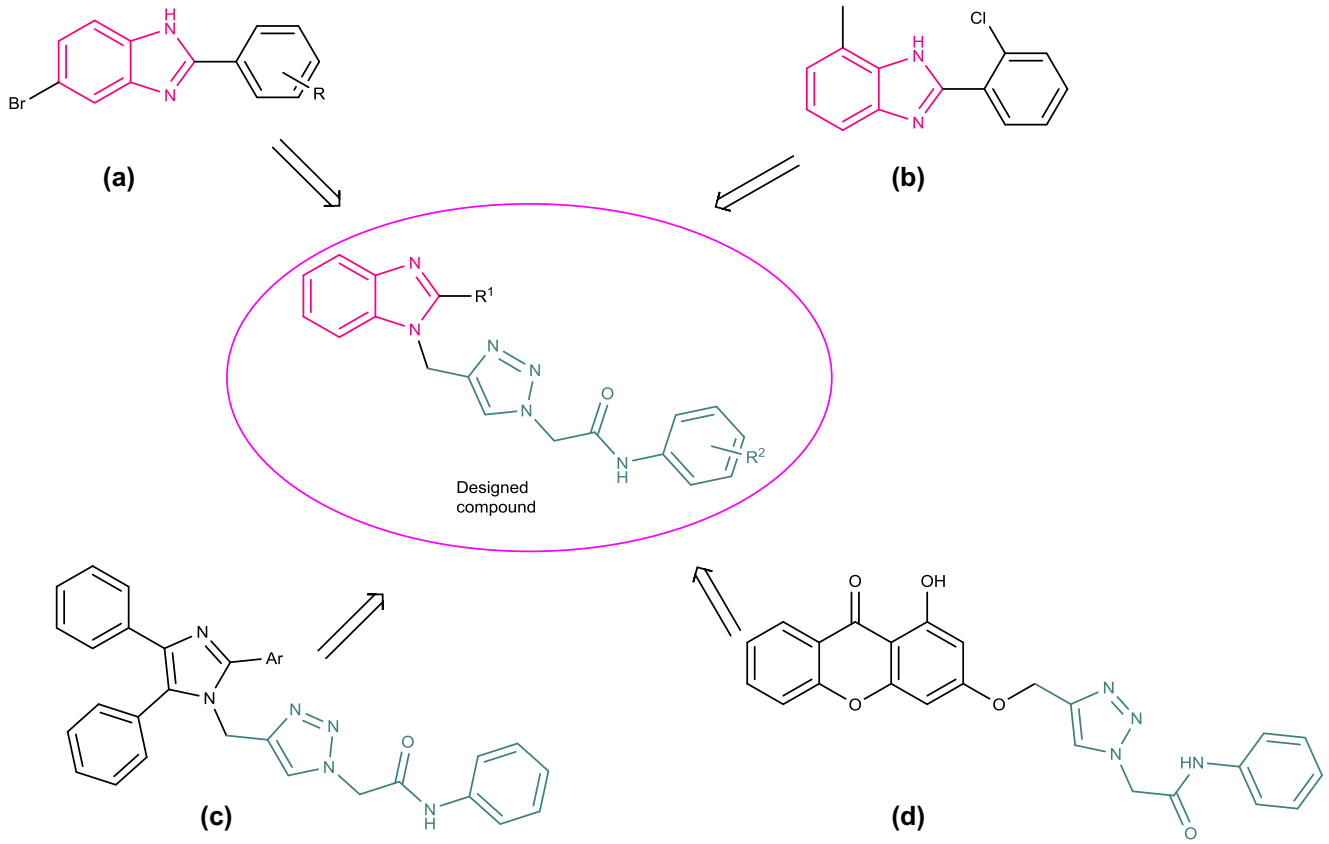

FIGURE 1 The design strategy for the benzimidazole-tethered 1,2,3-triazoles

benzimidazole–triazole hybrid as a potent antidiabetic agent, is reported in this study.

2 | RESULTS AND DISCUSSION

2.1 | Chemistry

A library of 18 compounds was synthesized in the current study. Compounds **1a,b** (Scheme 1) and 2-substituted 1-(prop-2-yn-1-yl)-1*H*-benzo[*d*]imidazoles **2a,b** were formed by using substituted benzimidazoles and propargyl bromide using the reported procedure.[23] The *N*-substituted 2-bromoacetamides **3a–i** were synthesized by reacting aniline derivatives and bromoacetyl bromide in tetrahydrofuran using triethylamine as a base.[31] Target compounds, substituted {4-[(1*H*-benzoimidazol-1-yl)methyl]-1*H*-1,2,3-triazol-1-yl}-acetamides (**4a–r**), were synthesized by Cu(I)-catalyzed Huisgen 1,3-dipolar cycloaddition reaction of alkyne and azide in which in situ azide was formed from *N*-substituted 2-bromoacetamides[23] (Scheme 2).

The structure of synthesized compounds was confirmed by various spectroscopic techniques, that is, one-dimensional nuclear magnetic resonance (NMR), two-dimensional (2D) NMR, Fourier transform infrared, and high-resolution mass spectra (HRMS). The formation of compounds **4a–r** was ascertained by the presence of two bands, that is, 1,600–1,620 cm^{-1} (amide I) and 1,680–1,695 cm^{-1} (amide II) in IR. In ^{1}H spectra, the characteristic NH peak was observed at δ 10.29–12.29, and another singlet was observed due to a triazole proton at δ 8.11–8.41. Two singlets for the methylene group attached to N_{16} of triazole ring and C_{13} of the triazole ring appeared in the region of δ 5.25–5.49 and 5.46–5.55, respectively. In ^{13}C NMR spectra of the compounds, signal due to C_{13} of the triazole moiety appeared at δ 142.94–143.48, whereas peak owing to C_{17} of triazole ring resonated at δ 125.66–125.56. The carbonyl carbon appeared at δ 164.00–165.53. The peaks of ^{1}H and ^{13}C spectrum were confirmed by correlating them with different types of correlation spectroscopy,

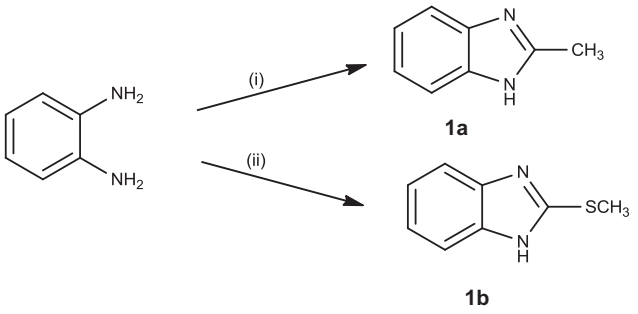

SCHEME 1 The synthesis of compounds **1a,b**. Reagents and conditions: (i) Acetic acid, reflux, 4–5 hr, (ii) (a) CS_2, KOH, ethanol; (b) CH_3I, ethanol

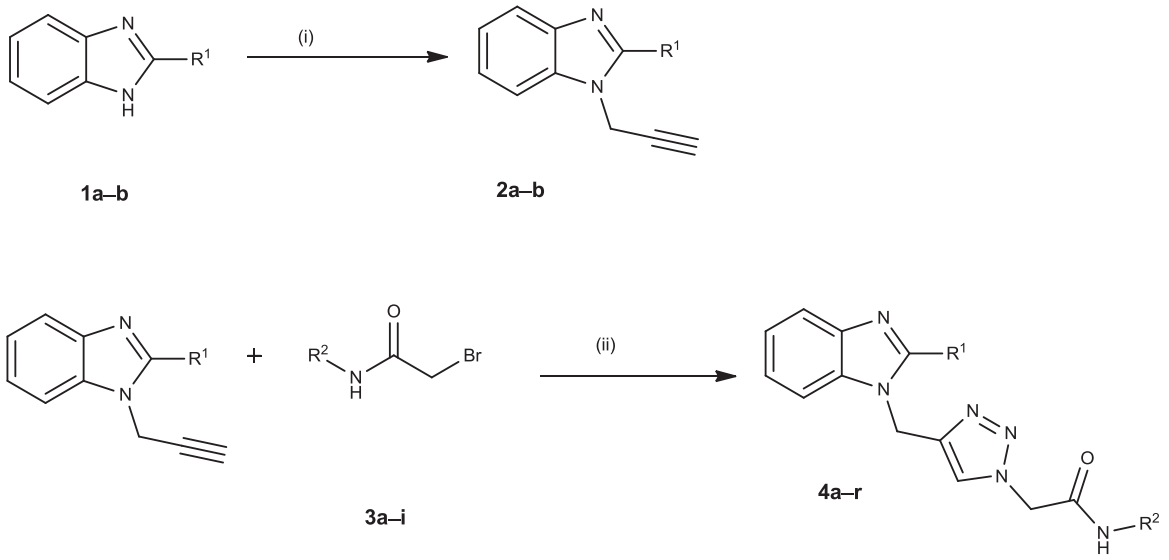

Comp.	R^1	R^2	Comp.	R^1	R^2
4a	$-CH_3$	$-C_6H_5$	**4j**	$-SCH_3$	$-C_6H_5$
4b	$-CH_3$	$-2-ClC_6H_4$	**4k**	$-SCH_3$	$-2-ClC_6H_4$
4c	$-CH_3$	$-2-NO_2C_6H_4$	**4l**	$-SCH_3$	$-2-NO_2C_6H_4$
4d	$-CH_3$	$-2-CH_3COC_6H_4$	**4m**	$-SCH_3$	$-2-CH_3COC_6H_4$
4e	$-CH_3$	$-3-FC_6H_4$	**4n**	$-SCH_3$	$-3-FC_6H_4$
4f	$-CH_3$	$-4-CH_3C_6H_4$	**4o**	$-SCH_3$	$-4-CH_3C_6H_4$
4g	$-CH_3$	$-4-OCH_3C_6H_4$	**4p**	$-SCH_3$	$-4-OCH_3C_6H_4$
4h	$-CH_3$	$-4-FC_6H_4$	**4q**	$-SCH_3$	$-4-FC_6H_4$
4i	$-CH_3$	$-1-C_{10}H_7$	**4r**	$-SCH_3$	$-1-C_{10}H_7$

SCHEME 2 The synthesis of compounds **4a–r**. Reagents and conditions: (i) K_2CO_3, propargyl bromide, DMF, 10–15°C, stirring 4–5 hr; (ii) NaN_3, $CuSO_4.5H_2O$, sodium ascorbate, DMF/H_2O (8:2), 50°C, stirring 5–6 hr

like correlation spectroscopy (COSY), total correlation spectroscopy (TOCSY), heteronuclear single-quantum coherence (HSQC), and heteronuclear multiple bond correlation (HMBC). The mass spectra of the compounds showed signals due to $[M^+]$ and $[M^+ + 1]$ ions, which were in good agreement with their calculated values.

In the ^1H spectra of compound **4j** (Figure 2), one singlet at δ 8.13 ppm was assigned as a triazole proton, that is, C_{17}–H. One doublet of doublets of one proton at 7.61 was due to C_6–H. The four triplets at δ 7.54, 7.56, 7.32, and 7.08 ppm were attributed to C_3–H, C_{22}–H/C_{26}–H, C_{23}–H/C_{25}–H, and C_{24}–H, respectively. Two protons (C_1–H and C_2–H) gave a multiplet at δ 7.18 ppm due to C_1–H and C_2–H, respectively. The above assignment was supported by 2D NMR, for example, COSY and TOCSY. The ^1H–^1H correlation between C_1–H/C_2–H and C_6–H, C_1–H/C_2–H and C_3–H, C_{22}–H/C_{26}–H and C_{23}–H/C_{25}–H, and C_{23}–H/C_{25}–H with both C_{22}–H/C_{26}–H and C_{24}–H was established through COSY spectrum. The TOCSY experiment suggested the correlation of C_3–H with C_1–H/C_2–H and C_6–H and C_{22}–H/C_{26}–H with C_{23}–H/C_{25}–H and C_{24}–H.

The ^{13}C NMR spectrum of compound **4j** (Figure 2) indicated the presence of 16 signals. Distortionless enhancement by polarization transfer ^{13}C NMR clearly indicated the presence of two secondary carbons and eight tertiary carbons, thereby suggesting that the remaining six are quaternary carbons. To establish the assignment of each carbon HSQC and HMBC, NMR experiments were carried out. HSQC revealed the assignment of carbon signals at δ 129.34 (C_{22}/C_{26}), 125.57 (C_{17}), 124.26 (C_{24}), 122.02 (C_1), 122.06 (C_2), 119.74 (C_{23}/C_{25}), 118.01 (C_6), 110.29 (C_3), 52.68 (C_{18}), 39.21 (C_{12}), and 14.93 (C_{11}), because the key correlation was as follows: δ 8.13 → 125.57, 7.61 → 110.29, 7.56 → 118.01, 7.54 → 129.34, 7.32 → 119.74, 7.18 → 122.06 and 122.02, and 7.08 → 124.26.

The HMBC experiment established the assignment of quaternary carbon signals through a two-bond correlation at δ 164.55 (C_{19}), 152.68 (C_8), 142.28 (C_5), 143.45 (C_{13}), 138.82 (C_{21}), and 136.57 (C_4). The above assignment was confirmed through HMBC; the HMBC correlation of signals is as follows: δ 5.46 → 152.68, 143.45, 136.57, and 125.57; 5.29 → 125.57 and 164.51; 7.08 → 119.74;

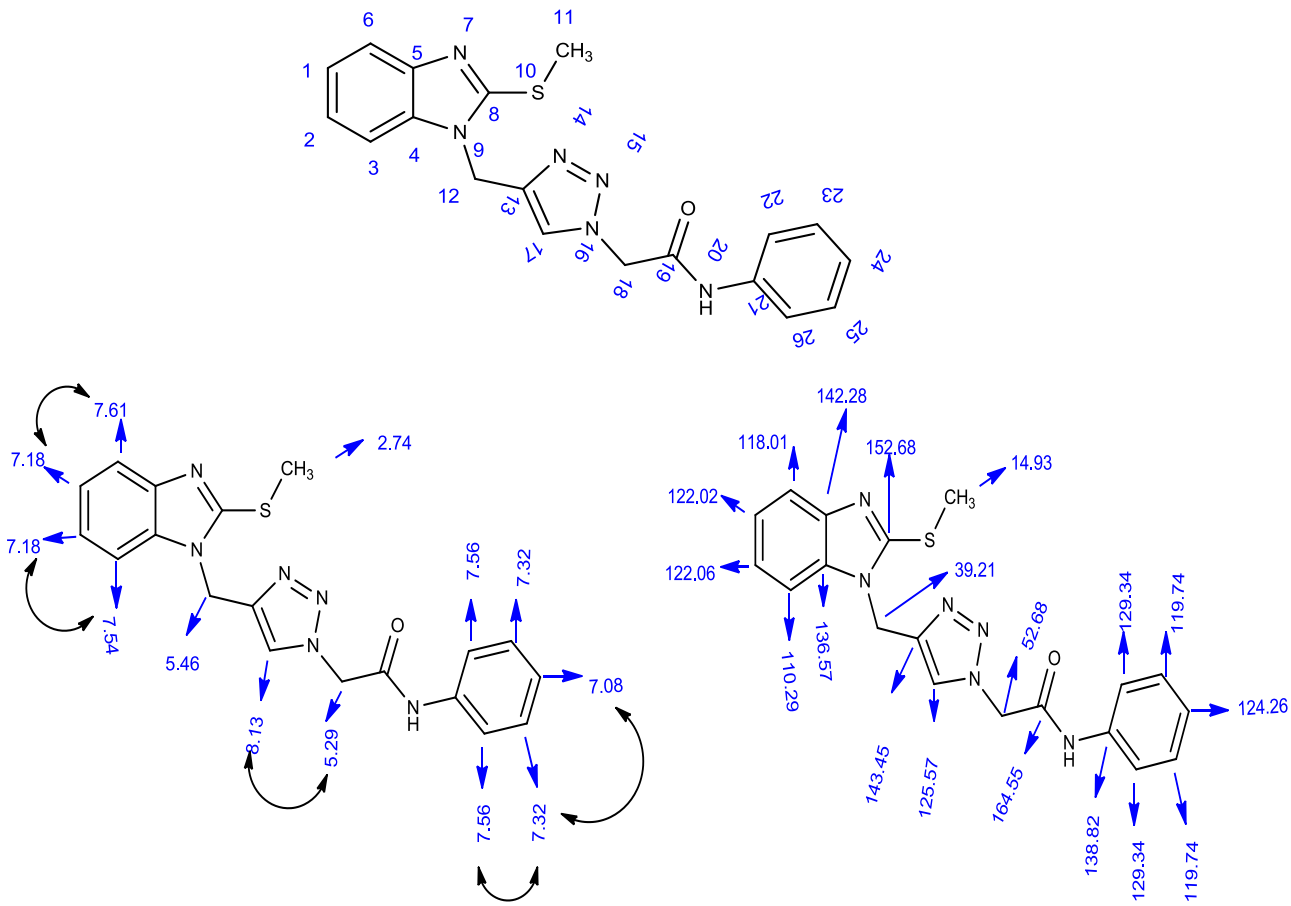

FIGURE 2 The structure and ^{1}H and ^{13}C nuclear magnetic resonance signals of compound **4j**

7.18 → 118.01; 7.32 → 138.82 and 129.34; 7.56 → 119.74 and 124.26; 7.61 → 122.02 and 122.06; 8.13 → 143.45.

2.2 | Pharmacology

2.2.1 | Inhibition of α-glucosidase and α-amylase

The inhibitory potential against α-glucosidase and α-amylase enzymes was tested using acarbose as a standard drug, and the IC_{50} values for both enzymes are listed in Table 1. All compounds showed inhibitory activity in the range of IC_{50} = 0.0410–0.0916 μmol/ml for α-amylase and IC_{50} = 0.0146–0.0732 μmol/ml for α-glucosidase, and compounds **4e**, **4g**, **4h**, **4n**, and **4p** were found to be good inhibitors.

In the case of α-amylase inhibition, F and OCH_3 group at R^2 substitution were more potent. Furthermore, F group at the *meta* position of the phenylacetamide ring was more active than F at *para* position, except in **4h**, and in α-glucosidase inhibition, the same trend was observed (Figure 3). The compounds with nonpolar substituents were less active as compared with a polar substituent. The structure–activity relationship of all the compounds (**4a–r**) showed that substitution at R_1 exhibited variable results. Compound **4n** was most active for α-amylase inhibition, with IC_{50} value 0.0410 μmol/ml, and compound **4e** was most active for α-glucosidase inhibition, with IC_{50} value 0.0146 μmol/ml.

2.3 | Molecular docking

To ascertain the binding conformation and interactions of the active compounds with the active site residues, docking simulations were carried out in the binding pocket of α-glucosidase. The most stable binding conformation of compounds **4e**, **4g**, and **4n** along with the interacting residues of the binding site is depicted in Figure 4.

Fluorine atom of the compound **4e** seemed to be very important for binding with the enzyme. This atom formed one hydrogen bond with His348 (green dots) and made two halogen bonds with Asp349 (light blue dots). Amide group NH created a hydrogen bond with oxygen atom of Glu276. π Orbitals of fluorophenyl ring had π–cation and π–anion interactions (yellow dots) with Arg439 and Asp214, respectively. π Orbitals of benzimidazole and triazole rings interacted with π electrons of Phe157 through interesting T-shaped π–π stacked interactions (pink dots). Similarly, compound **4g** displayed almost the same type of interactions, except that of fluorine atom of **4e**, as this is not present in **4g**. In compound **4n**, *m*-fluorine atom showed hydrogen bonding with

TABLE 1 IC_{50} values of compounds **4a–r**

S. No.	Compounds	α-Amylase inhibition		α-Glucosidase inhibition	
		IC_{50} value (μg/ml)	IC_{50} value (μmol/ml)	IC_{50} value (μg/ml)	IC_{50} value (μmol/ml)
1	**4a**	31.74	0.0916	20.95	0.0605
2	**4b**	20.1	0.0528	19.94	0.0524
3	**4c**	21.89	0.0559	15.55	0.0397
4	**4d**	26.75	0.0689	19.53	0.0503
5	**4e**	**19.44**	**0.0534**	**5.304**	**0.0146**
6	**4f**	32.54	0.0829	26.72	0.0681
7	**4g**	**16.88**	**0.0448**	**5.8**	**0.0154**
8	**4h**	**18.64**	0.0512	**9.76**	0.0268
9	**4i**	31.53	0.0795	29.03	0.0732
10	**4j**	31.89	0.0843	22.8	0.0602
11	**4k**	22.39	0.0542	18.67	0.0452
12	**4l**	24.82	0.0586	16.64	0.0393
13	**4m**	26.94	0.0641	13.09	0.0311
14	**4n**	**16.24**	**0.0410**	**6.44**	**0.0162**
15	**4o**	32.75	0.0834	25.48	0.0649
16	**4p**	**17.59**	**0.0431**	**8.18**	0.0200
17	**4q**	20.33	0.0513	**9.93**	0.0251
18	**4r**	31.41	0.0733	19.14	0.0447
19	Acarbose	15.31	0.0237	4.12	0.0064

Note: The high activity value is marked in bold.

His111 and Gln181, and formed a halogen bond with Asp68. The docking scores of these conformations were −10.4, −9.2, and −8.2 kcal/mol for compounds **4e**, **4g**, and **4n**, respectively. The experimental activity also followed the same order, that is, **4e** > **4g** > **4n**. Thus, these computational study results were in a good correlation with the experimental outcomes. Compounds went deep into the active site, whereas acarbose could not penetrate the active site deeply due to its larger size. A cartoon diagram of the protein along with docked acarbose and **4e**, **4g**, as well as **4n** is shown in Figure 5.

2.4 | Druglikeness of target compounds

Druglikeness refers to the similarity of the properties and structural features of the compounds with the known drug molecules. Some important properties to determine drug-likeness were calculated by Molinspiration property calculator (https://www.molinspiration.com). These properties give information about the bioavailability of organic compounds in the human body. Various properties calculated are listed in Table 2. It is interesting to note from the table that there is zero violation (Nviolation) of Lipinski's rule of five, so it can be inferred that all the target compounds follow this rule, that is, (a) the molecular weight is <500, (b) the calculated partition coefficient (miLogP) < 5, (c) <5 hydrogen bond donors (OH and NH moieties), and (d) <10 hydrogen bond acceptors (especially N and O). Thus, they are drug-like compounds that can be used orally.[32] Veber et al.[33] have suggested that the number of rotatable bonds should be less than 10 and the polar surface area should be less than 140 Å. All these synthesized molecules passed these criteria for good oral bioavailability. There is zero violation, which confirms the good drug-likeness of the synthesized molecules.

3 | CONCLUSION

Benzimidazole–1,2,3-triazoles, designed as a potential antidiabetic agent, were synthesized by employing a click reaction in DMF/H_2O in a good yield. The structure of the newly synthesized benzimidazole–1,2,3-triazoles was elucidated utilizing different spectroscopic techniques and they were found to exhibit a good antidiabetic activity. Compounds **4e**, **4g**, **4n**, and **4p** showed good inhibitory activity against α-amylase, and **4e, 4g**, and **4n** were found to be more potent against α-glucosidase. Furthermore, all the compounds displayed good absorption, distribution,

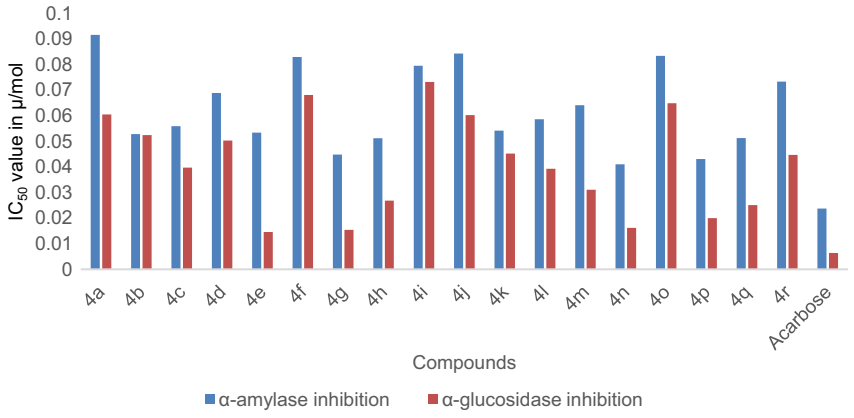

FIGURE 3 α-Amylase and α-glucosidase inhibitory activity of benzimidazole derivatives

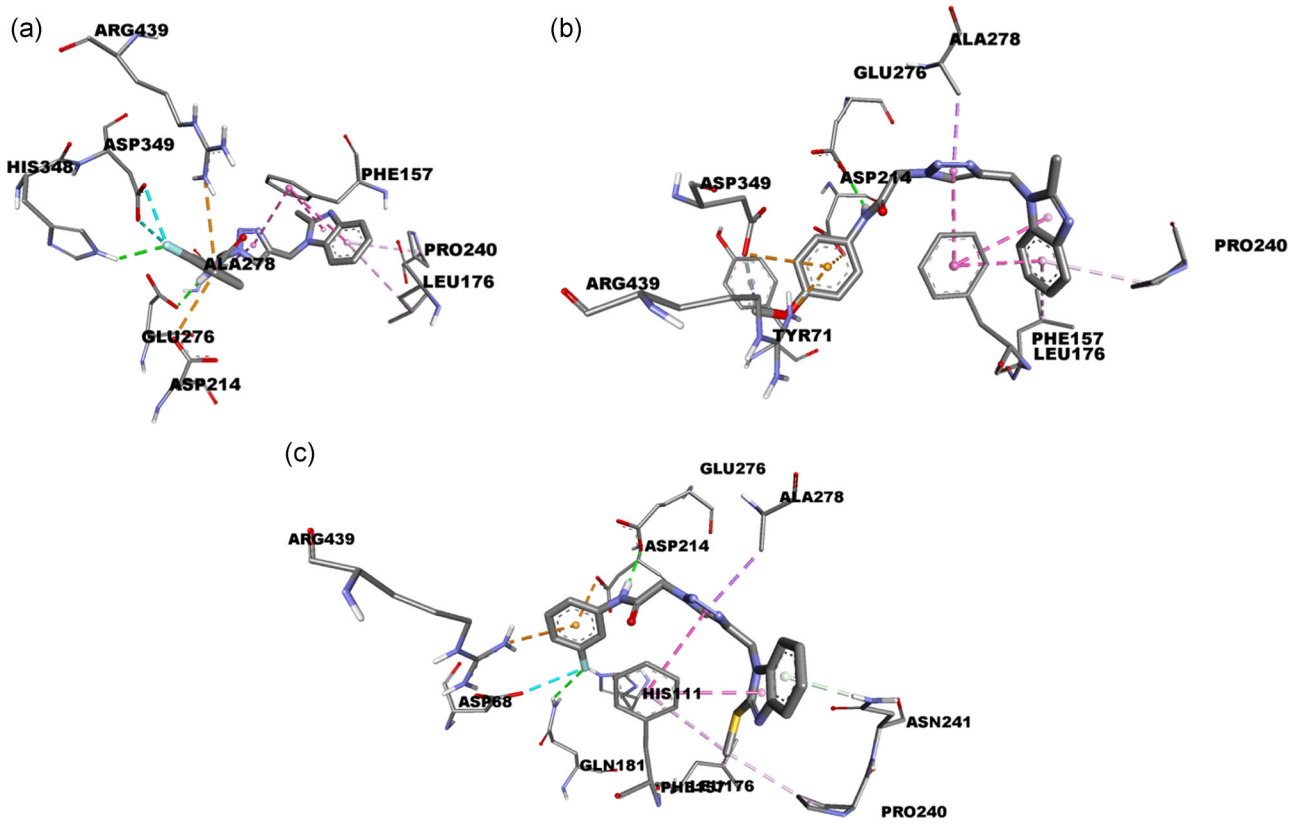

FIGURE 4 Binding interactions of compounds (a) **4e**, (b) **4g**, and (c) **4n** in the active site of α-glucosidase

metabolism, and excretion properties and zero violation of rules for drug-likeness. Docking studies showed that compound **4e** went deeper into the active site than acarbose, thereby effectively binding with the enzyme. In addition, it also revealed the role of hydrogen bonding, halogen bonding, and T-shaped π–π interactions with the active site residues, and the docking scores were well correlated with the experimental results. The correlation of docking score with in vitro results further supported the experimental results. The findings of the above investigations would certainly be helpful to the researchers working in the field of diabetes in designing better therapeutics, and these molecules may act as a good lead.

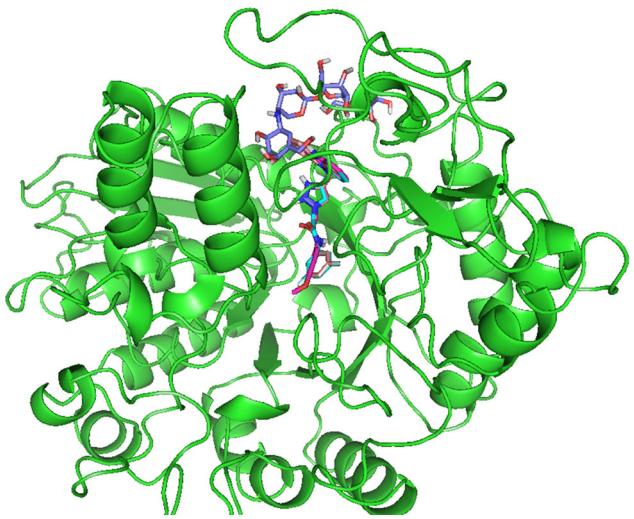

FIGURE 5 α-Glucosidase containing docked acarbose (blue) and compounds **4e** (cyan), **4g** (magenta), and **4n** (brown)

4 | EXPERIMENTAL

4.1 | Chemistry

4.1.1 | General

In the present study, chemicals were procured from Alfa Aesar/Sigma Aldrich and used as such without further purification. To detect the melting point of synthesized compounds, open capillary method was used. Standard literature procedures were used for drying the solvents. To perform thin-layer chromatography (TLC), precoated Merck silica gel (SIL G/UV254; ALUGRAM) plates were used in ethyl acetate/hexane mixture solvent system, followed by observing spots under ultraviolet light (254 nm). The ^{1}H NMR (400 MHz) and ^{13}C NMR (100 MHz) spectra were taken in dimethyl sulfoxide (DMSO)-d_6 by Bruker Avance III. The chemical shifts of DMSO for ^{1}H (δ 2.50 ppm) and ^{13}C (δ 39.50 ppm) were used as a reference. The IR spectra of synthesized compounds were recorded on Shimadzu IR Affinity-I using KBr powder as a standard in the region of 4,000–400 cm^{-1}. The HRMS were recorded by mass spectrometer Esquire 3000 with electrospray ionization (ESI) resources.

TABLE 2 Molinspiration properties

Compounds	miLogP	TPSA	N atoms	MW	nON	nOHNH	Nviolation	nRotB	Volume
4a	2.14	77.64	26	346.39	7	1	0	5	310.67
4b	2.77	77.64	27	380.84	7	1	0	5	324.20
4c	2.05	123.47	29	391.39	10	1	0	6	334
4d	1.99	94.71	29	388.43	8	1	0	6	346.21
4e	2.28	77.64	27	364.38	7	1	0	5	315.6
4f	3.42	77.64	28	392.49	7	1	0	6	345.36
4g	2.19	86.88	28	376.42	8	1	0	6	336.21
4h	2.3	77.64	27	364.38	7	1	0	5	315.6
4i	3.3	77.64	30	396.45	7	1	0	5	354.66
4j	2.97	77.64	27	378.46	7	1	0	6	328.8
4k	3.6	77.64	28	412.91	7	1	0	6	342.33
4l	2.88	123.47	30	423.46	10	1	0	7	352.13
4m	2.82	94.71	30	420.5	8	1	0	7	364.34
4n	3.11	77.64	28	396.45	7	1	0	6	333.73
4o	3.42	77.64	28	392.49	7	1	0	6	345.36
4p	3.02	86.88	29	408.49	8	1	0	7	354.34
4q	3.13	77.64	28	396.45	7	1	0	6	333.73
4r	4.13	77.64	31	428.52	7	1	0	6	372.79

Abbreviations: MW, molecular weight; miLogP, calculated partition coefficient; nRotB, number of rotatable bonds; TPSA, topological polar surface area.

The original spectra are provided as Supporting Information, as are the InChI codes of the investigated compounds, together with some biological activity data.

4.1.2 | Synthesis of 2-methyl-1*H*-benzimidazole (1a)

A synthetic method reported in the literature[34] was followed to synthesize **1a**. *o*-Phenylenediamine (12.5 g) was treated with 11.25 g of 90% acetic acid in a 250-ml round-bottom flask. The reaction mixture was heated at 100°C in a water bath for 2 hr. The reaction was monitored by TLC. After the completion of the reaction, the reaction mixture was cooled and a 10% sodium hydroxide solution was slowly added through mixing by continuous rotation of the flask until the reaction mixture was just alkaline to litmus and precipitate was formed. The precipitate was filtered, washed with ice-cold water, and then purified.

4.1.3 | Synthesis of 2-(methylthio)-1*H*-benzimidazole (1b)

2-(Methylthio)-1*H*-benzimidazole **1b** was synthesized by a two-step procedure according to an earlier reported method.[35] In a 250-ml round-bottom flask, *o*-phenylenediamine (2.0 g) was dissolved in absolute ethanol (50 ml) and then carbon disulfide (14 ml) was added. The reaction mixture was refluxed for 10 hr. Then the mixture was poured in a beaker and (10%) sodium hydroxide and some concentrated hydrochloric acid were added until the mixture became acidic to precipitate 2-mercaptobenzimidazole, which was filtered, dried, and then recrystallized from ethanol and water.

2-Mercaptobenzimidazole (2.0 g, 0.0133 mol) was dissolved in absolute ethanol (15 ml) with methyl iodide (0.0133 mol) and sodium hydroxide (0.53 g, 0.0133 mol) in a round flask (50 ml) with a reflux condenser. The reaction mixture was refluxed for 5 hr and filtered directly to get rid of the precipitated salt; the filtered sample was cooled and recrystallized from ethanol and water.

4.1.4 | Synthesis of 2-substituted 1-(prop-2-yn-1-yl)-1*H*-benzo[*d*]imidazoles (2a,b)

Potassium carbonate (4 mmol) was added to a solution of substituted benzimidazole (2 mmol) in 15 ml dimethylformamide, and the mixture was stirred for 10 min. Propargyl bromide (2.4 mmol) was added dropwise and the reaction mixture was stirred at 10–15°C for 4–5 hr.[23] The workup of the reaction was done with ice-cold water and the compound was extracted with ethyl acetate. The ethyl acetate layer was dried over anhydrous Na_2SO_4, filtered, and concentrated under vacuum to yield **2a,b**. The synthesized compounds were recrystallized with ethanol (spectroscopic data were in agreement with published data).

4.1.5 | Synthesis of *N*-substituted 2-bromoacetamides (3a–i)

The *N*-substituted 2-bromoacetamides **3a–i** were synthesized by an earlier reported method.[31] In a round-bottom flask, substituted aniline (1.0 mmol), bromoacetyl bromide (1.0 mmol) and triethylamine (1.1 mmol) were stirred in tetrahydrofuran at 0–10°C for 3–4 hr. The mixture was diluted with dichloromethane (50 ml), washed with saturated ammonium chloride solution, dried over anhydrous sodium sulfate. The excess of solvent was removed under reduced pressure and the obtained compound was crystallized from chloroform (spectroscopic data were in agreement with published data).

4.1.6 | Synthesis of substituted {4-[(1*H*-benzoimidazol-1-yl)methyl]-1*H*-1,2,3-triazol-1-yl}-acetamides (4a–r)

In a round-bottom flask, a mixture of 2-substituted 1-(prop-2-yn-1-yl)-1*H*-benzo[*d*]imidazoles **2a**,**b** (1.4 mmol), *N*-substituted 2-bromoacetamides **3a**–**i** (1.4 mmol), and sodium azide (2.8 mmol) was taken in dimethylformamide/water (8:2), and then copper sulfate pentahydrate (14 mol%) and sodium ascorbate (28 mol%) were added, and the reaction mixture was stirred for 5–6 hr at 50°C.[36–38] The reaction progress was monitored by TLC. After the completion of reaction, workup was done by adding ammonia solution and product was extracted with ethyl acetate (3 × 50 ml). The ethyl acetate layer was washed with brine solution and dried using anhydrous sodium sulfate. The solution was concentrated under reduced pressure and residue was purified by recrystallization with $CHCl_3$. The desired products, 1,2,3-triazole–benzimidazole hybrid, **4a–r**, were isolated in good yields.

*2-{4-[(2-Methyl-1*H*-benzo[*d*]imidazol-1-yl)methyl]-1*H*-1,2,3-triazol-1-yl}-*N*-phenylacetamide (**4a**)*

Yellow color, yield: 60%, M.P.: 158–160°C, ^{1}H NMR (400 MHz, DMSO) δ = 10.43 (s, 1H, N–H), 8.18 (s, 1H, C–H triazole), 7.64 (d, *J* = 8.1 Hz, 1H), 7.54 (t, *J* = 7.7 Hz, 2H), 7.52 (d, *J* = 7.7 Hz, 1H), 7.32 (t, *J* = 7.9 Hz, 2H), 7.16 (dt, *J* = 16.3, 6.8 Hz, 2H), 7.08 (t, *J* = 7.4 Hz, 1H), 5.53 (s, 2H), 5.28 (s, 2H), and 2.67 (s, 3H, CH_3). ^{13}C NMR (100 MHz, DMSO) δ = 164.57 (C═O), 152.19, 142.96 (C_{13} triazole), 142.73, 138.82, 135.39, 129.38, 125.58 (C_{17} triazole), 124.25, 121.98, 121.76, 119.66, 118.67, 110.52, 52.64, 38.57, and 14.22. (KBr, υ_{max}) = 3,305 (N–H str.), 3,140 (C–H str., triazole), 3,051 (C–H str., aromatic), 1,697 (C═O str. amide), 1,616 (N–H bending), 1,558, 1,519, and 1,492 (C═C str., aromatic) cm^{-1}. HRMS (ESI): *m/z* calculated for $[M+H]^+$ $C_{19}H_{18}N_6O$ 347.1620; found 347.1617.

N-*(2-Chlorophenyl)-2-{4-[(2-methyl-1*H*-benzo[*d*]imidazol-1-yl)-methyl]-1*H*-1,2,3-triazol-1-yl}acetamide (**4b**)*

Yellow color, yield: 63%, M.P.: 156°C, ^{1}H NMR (400 MHz, DMSO) δ = 10.58 (s, 1H, N–H), 8.18 (s, 1H, C–H triazole), 7.65 (d, *J* = 8.1 Hz, 1H), 7.58 (d, *J* = 8.8 Hz, 2H), 7.52 (d, *J* = 7.4 Hz, 1H), 7.38 (d, *J* = 8.8 Hz, 2H), 7.21–7.13 (m, 2H), 5.54 (s, 2H), 5.29 (s, 2H), and 2.67 (s, 3H, CH_3). ^{13}C NMR (100 MHz, DMSO) δ = 164.79 (C═O), 142.96 (C_{13} triazole), 137.79, 129.31, 127.82, 125.60 (C_{17} triazole), 122.03, 121.80, 121.23, 118.63, 110.59, 63.74, 52.63, 38.62, and 14.24. IR (KBr, υ_{max}) = 3,251 (N–H str.), 3,135 (C–H str., triazole), 3,030 (C–H str., aromatic), 1,695 (C═O str.), 1,622 (N–H bending), 1,556, 1,514, and 1,458 (C═C str., aromatic) cm^{-1}. HRMS (ESI): *m/z* calculated for $[M+H]^+$ $C_{19}H_{17}N_6ClO$ 381.1231; found 381.1229.

*2-{4-[(2-Methyl-1*H*-benzo[*d*]imidazol-1-yl)methyl]-1*H*-1,2,3-triazol-1-yl}-*N*-(2-nitrophenyl)acetamide (**4c**)*

Green color, yield: 58%, M.P.: 148–150°C, ^{1}H NMR (400 MHz, DMSO) δ = 10.73 (s, 1H, N–H), 8.16 (s, 1H, C–H triazole), 7.98 (d, *J* = 7.8 Hz, 1H), 7.82–7.64 (m, 3H), 7.58 (s, 1H), 7.41 (t, *J* = 7.0 Hz, 1H), 7.17 (d, *J* = 7.1 Hz, 2H), 5.55 (s, 2H), 5.37 (s, 2H), and 2.65 (s, 3H, CH_3). ^{13}C NMR (100 MHz, DMSO) δ = 165.34 (C═O), 143.02 (C_{13} triazole), 142.88, 134.64, 130.74, 126.39, 126.02, 125.53 (C_{17} triazole), 122.02, 121.78, 118.63, 110.63, 52.39, 38.64, and 14.23. IR (KBr, υ_{max}) = 3,286 (N–H str.), 3,145 (C–H str., triazole), 3,053 (C–H str., aromatic), 1,691 (C═O str. amide), 1,608 (N–H bending), 1,553, 1,502, and 1,465 (C═C str., aromatic) cm^{-1}. HRMS (ESI): *m/z* calculated for $[M+H]^+$ $C_{19}H_{17}N_7O_3$ 392.1471; found 392.1569.

N-*(2-Acetylphenyl)-2-{4-[(2-methyl-1*H*-benzo[*d*]imidazol-1-yl)-methyl]-1*H*-1,2,3-triazol-1-yl}acetamide (**4d**)*

White color, yield: 54%, M.P.: 124–126°C, ^{1}H NMR (400 MHz, DMSO) δ = 12.29 (s, 1H, N–H), 8.41 (s, 1H, C–H triazole), 7.89 (d, *J* = 8.0 Hz, 1H), 7.66 (t, *J* = 7.8 Hz, 2H), 7.54 (d, *J* = 7.5 Hz, 1H), 7.42 (d, *J* = 8.1 Hz, 1H), 7.32 (t, *J* = 7.6 Hz, 1H), 7.28–7.08 (m, 2H), 5.61 (s, 2H), 5.39 (s, 2H), 2.70 (s, 3H, CH_3), and 2.15 (s, 3H, CH_3). ^{13}C NMR (100 MHz, DMSO) δ = 202.77 (carbonyl carbon), 165.58, 143.32, 142.79 (C_{13} triazole), 138.32, 134.60, 132.02, 125.48 (C_{17} triazole), 124.26, 121.92, 121.71, 121.42, 118.53, 110.50, 53.26, 38.59, 29.03, and 14.29. IR (KBr, υ_{max}) = 3201 (N–H str.), 3,130 (C–H str., triazole), 3,076 (C–H str., aromatic), 1,720 (C═O str.), 1,641 (N–H bending), 1,608, 1,559, 1,531, and 1,465 (C–C str., aromatic) cm^{-1}. HRMS (ESI): *m/z* calculated for $[M+H]^+$ $C_{21}H_{20}N_6O_2$ 389.1726; found 389.1723.

N-*(3-Fluorophenyl)-2-{4-[(2-methyl-1*H*-benzo[*d*]imidazol-1-yl)-methyl]-1*H*-1,2,3-triazol-1-yl}acetamide (**4e**)*

Brown color, yield: 74%, M.P.: 155–156°C, ^{1}H NMR (400 MHz, DMSO) δ = 10.67 (s, 1H, N–H), 8.19 (s, 1H, C–H triazole), 7.66 (d, *J* = 7.1 Hz, 1H), 7.53 (d, *J* = 9.6 Hz, 2H), 7.37 (dd, *J* = 15.0, 8.0 Hz, 1H), 7.28 (d, *J* = 8.2 Hz, 1H), 7.18 (dd, *J* = 16.4, 8.6 Hz, 2H), 6.92 (t, *J* = 9.4 Hz, 1H), 5.54 (s, 2H), 5.31 (s, 2H), and 2.67 (s, 3H, CH_3). ^{13}C NMR (100 MHz, DMSO) δ = 165.03 (C═O), 162.58 (d, *J* = 241 Hz), 142.97 (C_{13} triazole), 140.51 (d, *J* = 11 Hz), 131.80 (d, *J* = 9 Hz), 125.59 (C_{17} triazole), 122.00, 121.75, 118.68, 115.44, 111.24, 110.86, 110.75 (d, *J* = 21 Hz), 106.52 (d, *J* = 26 Hz), 52.64, 38.65, and 14.27. IR (KBr, υ_{max}) = 3,292 (N–H str.), 3,140 (C–H str., triazole), 3,035 (C–H str., aromatic), 1,691 (C═O str.), 1,614 (N–H bending), 1,556, 1,514, and 1,470 (C═C str., aromatic) cm^{-1}. HRMS (ESI): *m/z* calculated for $[M+H]^+$ $C_{19}H_{17}N_6OF$ 365.1526; found 365.1529.

*2-{4-[(2-Methyl-1H-benzo[d]imidazol-1-yl)methyl]-1H-1,2,3-triazol-1-yl}-N-(p-tolyl)acetamide (**4f**)*

White color, yield: 74%, M.P.: 130–132°C, ^{1}H NMR (400 MHz, DMSO) δ = 10.34 (s, 1H, N–H), 8.17 (s, 1H, C–H triazole), 7.64 (d, *J* = 8.1 Hz, 1H), 7.52 (d, *J* = 7.2 Hz, 1H), 7.44 (d, *J* = 8.4 Hz, 2H), 7.22–7.09 (m, 4H), 5.53 (s, 2H), 5.26 (s, 2H), 2.67 (s, 3H, CH_3), and 2.25 (s, 3H, CH_3). ^{13}C NMR (100 MHz, DMSO) δ = 164.30 (C═O), 152.18, 142.94 (C_{13} triazole), 142.76, 136.41, 136.34, 135.40, 133.20, 129.74, 125.56 (C_{17} triazole), 121.96, 121.74, 119.65, 118.64, 110.51, 52.62, 38.57, 20.91, and 14.23. IR (KBr, υ_{max}) = 3,255 (N–H str.), 3,136 (C–H str., triazole), 3,037 (C–H str., aromatic), 1,693 (C═O str.), 1,618 (N–H bending), 1,556, 1,512, and 1,454 (C═C str., aromatic) cm^{-1}. HRMS (ESI): *m/z* calculated for $[M+H]^+$ $C_{20}H_{20}N_6O$ 361.1777; found 361.1759.

*N-(4-Methoxyphenyl)-2-{4-[(2-methyl-1H-benzo[d]imidazol-1-yl)-methyl]-1H-1,2,3-triazol-1-yl}acetamide (**4g**)*

Yellow color, yield: 84%, M.P.: 124–126°C, ^{1}H NMR (400 MHz, DMSO) δ = 10.30 (s, 1H, NH), 8.18 (s, 1H, C–H triazole), 7.64 (d, *J* = 7.6 Hz, 1H), 7.52 (d, *J* = 7.6 Hz, 1H), 7.47 (d, *J* = 8.9 Hz, 2H), 7.23–7.10 (m, 2H), 6.90 (d, *J* = 9.0 Hz, 2H), 5.53 (s, 2H), 5.25 (s, 2H), 3.33 (s, 3H, CH_3), and 2.67 (s, 3H, CH_3). ^{13}C NMR (100 MHz, DMSO) δ = 164.03 (C═O), 155.99, 152.18, 142.94 (C_{13} triazole), 142.73, 135.40, 131.94, 125.56 (C_{17} triazole), 121.97, 121.76, 121.21, 118.64, 114.42, 110.53, 55.63, 52.57, 38.58, and 14.24. IR (KBr, υ_{max}) = 3,251 (N–H str.), 3,140 (C–H str., triazole), 3,034 (C–H str., aromatic), 1,691 (C═O str.), 1,610 (N–H bending), 1,560, 1,510, and 1,460 (C═C str., aromatic) cm^{-1}. HRMS (ESI): *m/z* calculated for $[M+H]^+$ $C_{20}H_{20}N_6O_2$ 377.1726; found 377.1467.

*N-(4-Fluorophenyl)-2-{4-[(2-methyl-1H-benzo[d]imidazol-1-yl)-methyl]-1H-1,2,3-triazol-1-yl}acetamide (**4h**)*

Gray color, yield: 85%, M.P.: 180–182°C, ^{1}H NMR (400 MHz, DMSO) δ = 10.51 (s, 1H, N–H), 8.14 (s, 1H, C–H triazole), 7.72–7.38 (m, 4H), 7.29–7.07 (m, 4H), 5.47 (s, 2H), 5.29 (s, 2H), and 2.74 (s, 3H, CH_3). ^{13}C NMR (100 MHz, DMSO) δ = 164.51 (C═O), 158.69 (d, *J* = 239 Hz), 152.68, 143.46 (C_{13} triazole), 142.29, 136.55, 135.23 (d, *J* = 3 Hz), 125.63 (C_{17} triazole), 122.03 (d, *J* = 2 Hz), 121.47 (d, *J* = 8 Hz), 117.99, 115.98 (d, *J* = 22 Hz), 110.30, 52.56, 39.15, and 14.89. (KBr, υ_{max}) = 3,331 (N–H str.), 3,136 (C–H str., triazole), 3,070 (C–H str., aromatic), 1,690 (C═O str. amide), 1,616 (N–H bending), 1,563, 1,508, and 1,477 (C═C str., aromatic) cm^{-1}. HRMS (ESI): *m/z* calculated for $[M+H]^+$ $C_{19}H_{17}N_6OF$ 365.1526; found 365.1525.

*2-{4-[(2-Methyl-1H-benzo[d]imidazol-1-yl)methyl]-1H-1,2,3-triazol-1-yl}-N-(naphthalen-1-yl)acetamide (**4i**)*

White color, yield: 66%, M.P.: 145–147°C, ^{1}H NMR (400 MHz, DMSO) δ = 10.43 (s, 1H, N–H), 8.23 (s, 1H, C–H triazole), 8.11 (d, *J* = 9.0 Hz, 1H), 7.95 (d, *J* = 9.3 Hz, 1H), 7.79 (d, *J* = 8.2 Hz, 1H), 7.65 (t, *J* = 8.6 Hz, 2H), 7.58–7.47 (m, 4H), 7.22–7.11 (m, 2H), 5.54 (s, 2H), 5.49 (s, 2H), and 2.67 (s, 3H, CH_3). ^{13}C NMR (100 MHz, DMSO) δ = 165.53 (C–O), 142.97 (C_{13} triazole), 134.15, 133.08, 128.67, 128.02, 126.68, 126.52, 126.23, 126.04, 125.62 (C_{17} triazole), 123.70, 123.00, 122.11, 122.03, 121.82, 110.53, 52.51, 38.61, and 14.19. IR (KBr, υ_{max}) = 3,246 (N–H str.), 3,143 (C–H str., triazole), 3,055 (C–H str., aromatic), 1,691 (C═O str.), 1,616 (N–H bending), 1,556, 1,508, and 1,465 (C═C str., aromatic) cm^{-1}. HRMS (ESI): *m/z* calculated for $[M+H]^+$ $C_{23}H_{20}N_6O$ 397.1777; found 397.1773.

*2-{4-{[2-(Methylthio)-1H-benzo[d]imidazol-1-yl]methyl}-1H-1,2,3-triazol-1-yl}-N-phenylacetamide (**4j**)*

White color, yield: 74%, M.P.: 138–140°C, ^{1}H NMR (400 MHz, DMSO) δ = 10.41 (s, 1H, N–H), 8.13 (s, 1H, C–H triazole), 7.60 (d, *J* = 8.7 Hz, 1H), 7.56 (t, *J* = 8 Hz, 1H), 7.54 (d, *J* = 6.3 Hz, 2H), 7.32 (t, *J* = 7.9 Hz, 2H), 7.21–7.13 (m, 2H), 7.08 (t, *J* = 7.4 Hz, 1H), 5.46 (s, 2H), 5.28 (s, 2H), and 2.74 (s, 3H, CH_3). ^{13}C NMR (100 MHz, DMSO) δ = 164.50 (C═O), 152.68, 143.50 (C_{13} triazole), 142.28, 138.82, 136.57, 129.34, 125.57 (C_{17} triazole), 124.25, 122.06, 122.02, 119.74, 118.00, 110.21, 52.68, 39.21, and 14.93. (KBr, υ_{max}) = 3,267 (N–H str.), 3,142 (C–H str., triazole), 3,051 (C–H str., aromatic), 1,691 (C═O str. amide), 1,662 (N–H bending), 1,604, 1,558, and 1,442 (C═C str., aromatic) cm^{-1}. HRMS (ESI): *m/z* calculated for $[M+H]^+$ $C_{19}H_{18}N_6SO$ 379.1341; found 379.1342.

*N-(2-Chlorophenyl)-2-{4-{[2-(methylthio)-1H-benzo[d]imidazol-1-yl]methyl}-1H-1,2,3-triazol-1-yl}acetamide (**4k**)*

White color, yield: 67%, M.P.: 160–162°C, ^{1}H NMR (400 MHz, DMSO) δ = 10.57 (s, 1H, N–H), 8.13 (s, 1H, C–H triazole), 7.61–7.53 (m, 4H), 7.39–7.37 (m, 2H), 7.19–7.16 (m, 2H), 5.47 (s, 2H), 5.30 (s, 2H), and 2.74 (s, 3H, CH_3). ^{13}C NMR (100 MHz, DMSO) δ = 164.76 (C═O), 152.69, 143.46 (C_{13} triazole), 142.30, 137.79, 136.55, 127.82, 125.63 (C_{17} triazole), 122.05, 121.24, 117.99, 110.29, 52.62, 39.15, and 14.90. IR (KBr, υ_{max}) = 3338 (N–H str.), 3,134 (C–H str., triazole), 3,061 (C–H str., aromatic), 1,687 (C═O str.), 1,604 (N–H bending), 1,552, 1,492, and 1,446 (C═C str., aromatic) cm^{-1}. HRMS (ESI): *m/z* calculated for $[M+H]^+$ $C_{19}H_{17}N_6SClO$ 413.0951; found 413.0943.

*2-{4-{[2-(Methylthio)-1H-benzo[d]imidazol-1-yl]methyl}-1H-1,2,3-triazol-1-yl}-N-(2-nitrophenyl)acetamide (**4l**)*

Yellow color, yield: 65%, M.P.: 210–212°C, ^{1}H NMR (400 MHz, DMSO) δ = 10.70 (s, 1H, N–H), 8.11 (s, 1H, C–H triazole), 7.98 (dd, *J* = 8.2, 1.3 Hz, 1H), 7.72 (dd, *J* = 7.1, 1.4 Hz, 1H), 7.69 (d, *J* = 1.5 Hz, 1H), 7.59 (dd, *J* = 6.2, 2.7 Hz, 1H), 7.57–7.51 (m, 1H), 7.45–7.37 (m, 1H), 7.22–7.12 (m, 2H), 5.46 (s, 2H), 5.37 (s, 2H), and 2.73 (s, 3H, CH_3). ^{13}C NMR (100 MHz, DMSO) δ = 165.33 (C═O), 152.68, 143.46 (C_{13} triazole), 142.85, 142.37, 136.55, 134.63, 130.79, 126.36, 126.02, 125.61, 125.53, 122.04 (C_{17} triazole), 117.98, 110.29, 52.39, 39.13, and 14.89. IR (KBr, υ_{max}) = 3,329 (N–H str.), 3,142 (C–H str., triazole), 3,068 (C–H str., aromatic), 1,720 (C═O str.), 1,602 (N–H bending), 1,548, 1,492, and 1,442 (C═C str., aromatic) cm^{-1}. HRMS (ESI): *m/z* calculated for $[M+H]^+$ $C_{19}H_{17}N_7O_3S$ 424.1192; found 424.1182.

N-*(2-Acetylphenyl)-2-{4-{[2-(methylthio)-1*H*-benzo[d]imidazol-1-yl] methyl}-1*H*-1,2,3-triazol-1-yl}acetamide (**4m**)*

Gray color, yield: 53%, M.P.: 140–142°C, ^{1}H NMR (400 MHz, DMSO) δ = 11.33 (s, 1H, N–H), 8.22 (d, *J* = 8.3 Hz, 1H), 8.16 (s, 1H, C–H triazole), 7.99 (d, *J* = 6.7 Hz, 1H), 7.65–7.54 (m, 3H), 7.28–7.17 (m, 3H), 5.48 (s, 2H), 5.41 (s, 2H), 2.74 (s, 3H, CH_3), and 2.57 (s, 3H, CH_3). ^{13}C NMR (100 MHz, DMSO) δ = 202.73 (C═O), 165.53 (C═O, amide), 152.70, 143.46 (C_{13} triazole), 142.57, 138.27, 136.56, 134.56, 131.97, 125.60 (C_{17} triazole), 125.47, 124.28, 122.04, 122.02, 121.49, 117.97, 110.31, 53.23, 39.18, 29.06, and 14.91. IR (KBr, υ_{max}) = 3,318 (N–H str.), 3,136 (C–H str., triazole), 3,066 (C–H str., aromatic), 1,762 (C═O str. ketone), 1,687 (C═O str. amide), 1,581 (N–H bending), 1,521, 1,487, and 1,419 (C═C str., aromatic) cm^{-1}. HRMS (ESI): *m/z* calculated for $[M+H]^+$ $C_{21}H_{20}N_6SO_2$ 421.1447; found 421.1445.

N-*(3-Fluorophenyl)-2-{4-{[2-(methylthio)-1*H*-benzo[d]imidazol-1-yl]methyl}-1*H*-1,2,3-triazol-1-yl}acetamide (**4n**)*

White color, yield: 64%, M.P.: 160–162°C, ^{1}H NMR (400 MHz, DMSO) δ = 10.68 (s, 1H, N–H), 8.15 (s, 1H, C–H triazole), 7.61 (s, 1H), 7.55 (s, 2H), 7.38 (d, *J* = 14 Hz, 1H), 7.28 (d, *J* = 14 Hz, 1H), 7.18 (s, 2H), 6.93 (s, 1H), 5.47 (s, 2H), 5.32 (s, 2H), and 2.75 (s, 3H, CH_3). ^{13}C NMR (100 MHz, DMSO) δ = 165.02 (C═O), 162.58 (d, *J* = 243 Hz), 152.69, 143.46 (C_{13} triazole), 142.32, 140.52 (d, *J* = 11 Hz), 136.55, 131.09 (d, *J* = 9 Hz), 125.66, 122.03 (C_{17} triazole), 117.99, 115.42, 110.74 (d, *J* = 21 Hz), 110.30, 106.49 (d, *J* = 26 Hz), 52.62, 39.13, and 14.89. IR (KBr, υ_{max}) = 3,251 (N–H str.), 3,140 (C–H str., triazole), 3,034 (C–H str., aromatic), 1,691 (C═O str.), 1,610 (N–H bending), 1,560, 1,510, and 1,460 (C═C str., aromatic) cm^{-1}. HRMS (ESI): *m/z* calculated for $[M+H]^+$ $C_{19}H_{17}N_6SOF$ 397.1247; found 397.1249.

*2-{4-{[2-(Methylthio)-1*H*-benzo[d]imidazol-1-yl]methyl}-1*H*-1,2,3-triazol-1-yl}-*N*-(p-tolyl)acetamide (**4o**)*

White color, yield: 64%, M.P.: 124–126°C, ^{1}H NMR (400 MHz, DMSO) = 10.34 (s, 1H, N–H), 8.13 (s, 1H, C–H triazole), 7.61–7.42 (m, 4H), 7.20–711 (m, 4H), 5.46 (s, 2H), 5.26 (s, 2H), 2.74 (s, 3H, CH_3), and 2.25 (s, 3H, CH_3). ^{13}C NMR (100 MHz, DMSO) = 164.27 (C═O), 152.68, 143.47 (C_{13} triazole), 142.25, 136.58, 133.21, 129.73, 125.61 (C_{17} triazole), 122.05, 119.66, 117.99, 110.33, 52.62, 39.16, 20.90, and 14.90. IR (KBr, υ_{max}) = 3,271 (N–H Str.), 3,136 (C–H str., triazole), 3,059 (C–H str., aromatic), 1,691 (C═O str.), 1,612 (N–H bending), 1,554, 1,514, and 1,452 (C═C str., aromatic) cm^{-1}. HRMS (ESI): *m/z* calculated for $[M+H]^+$ $C_{20}H_{20}N_6OS$ 393.1498; found 393.1484.

N-*(4-Methoxyphenyl)-2-{4-{[2-(methylthio)-1*H*-benzo[d]imidazol-1-yl]methyl}-1*H*-1,2,3-triazol-1-yl}acetamide (**4p**)*

Gray color, yield: 63%, M.P.: 137–139°C, ^{1}H NMR (400 MHz, DMSO) δ = 10.29 (s, 1H, N–H), 8.13 (s, 1H, C–H triazole), 7.61–7.45 (m, 4H), 7.1–7.15 (m, 4H), 5.46 (s, 2H), 5.25 (s, 2H), 3.72 (s, 3H, CH_3), and 2.74 (s, 3H, CH_3). ^{13}C NMR (100 MHz, DMSO) δ = 164.00 (C═O), 155.99, 152.69, 143.46 (C_{13} triazole), 142.25, 136.55, 131.93, 125.61 (C_{17} triazole), 122.05, 121.21, 117.98, 114.46, 110.31, 55.63, 52.56, 39.15, 14.89. IR (KBr, υ_{max}) = 3,290 (N–H str.), 3,147 (C–H str., triazole), 3,003 (C–H str., aromatic), 1,687 (C═O str.), 1,614 (N–H bending), 1,556, 1,514, and 1,460 (C═C str., aromatic) cm^{-1}. HRMS (ESI): *m/z* calculated for $[M+H]^+$ $C_{20}H_{20}N_6SO_2$ 409.1447; found 409.1404.

N-*(4-Fluorophenyl)-2-{4-{[2-(methylthio)-1*H*-benzo[d]imidazol-1-yl]methyl}-1*H*-1,2,3-triazol-1-yl}acetamide (**4q**)*

Gray color, yield: 84%, M.P.: 170–172°C, ^{1}H NMR (400 MHz, DMSO) δ = 10.52 (s, 1H, N–H), 8.18 (s, 1H, C–H triazole), 7.64 (d, *J* = 7.5 Hz, 1H), 7.57 (dd, *J* = 9.1, 5.0 Hz, 2H), 7.52 (d, *J* = 7.5 Hz, 1H), 7.16 (ddt, *J* = 15.1, 9.8, 4.9 Hz, 4H), 5.53 (s, 2H), 5.28 (s, 2H), and 2.67 (s, 3H, CH_3). ^{13}C NMR (100 MHz, DMSO) δ = 164.53 (C═O), 158.69 (d, *J* = 239 Hz), 142.98 (C_{13} triazole), 135.23 (d, *J* = 3 Hz), 125.57 (C_{17} triazole), 121.84 (d, *J* = 21 Hz), 121.47 (d, *J* = 7 Hz), 118.65, 115.98 (d, *J* = 22 Hz), 110.51, 52.57, 38.57, and 14.23. IR (KBr, υ_{max}) = 3,261 (N–H Str.), 3,145 (C–H str., triazole), 3,037 (C–H str., aromatic), 1,691 (C═O str. amide), 1,622 (N–H bending), 1,571, 1,508, and 1,462 (C═C str., aromatic) cm^{-1}. HRMS (ESI): *m/z* calculated for $[M+H]^+$ $C_{19}H_{17}N_6SOF$ 397.1247; found 397.1249.

*2-{4-{[2-(Methylthio)-1*H*-benzo[d]imidazol-1-yl]methyl}-1*H*-1,2,3-triazol-1-yl}-N-(naphthalen-1-yl)acetamide (**4r**)*

White color, yield: 83%, M.P.: 151–153°C, ^{1}H NMR (400 MHz, DMSO) δ = 10.39 (s, 1H, N–H), 8.18 (s, 1H, C–H triazole), 8.13 (d, *J* = 8 Hz, 1H), 7.97–7.95 (m, 1H), 7.80 (d, *J* = 8.2 Hz, 1H), 7.69 (d, *J* = 8 Hz, 1H), 7.63–7.53 (m, 4H), 7.49 (t, *J* = 12 Hz, 1H), 7.19–7.16 (m, 2H), 5.49 (s, 2H), 5.48 (s, 2H), and 2.74 (s, 3H, CH_3). ^{13}C NMR (100 MHz, DMSO) δ = 165.50 (C═O), 152.69, 143.47 (C_{13} triazole), 142.31, 136.57, 134.16, 133.15, 128.66, 128.00, 126.65, 126.48, 126.17, 126.03, 125.66 (C_{17} triazole), 123.04, 122.02, 117.99, 110.31, 52.54, 39.18, and 14.90. IR (KBr, υ_{max}) = 3,340 (N–H str.), 3,136 (C–H str., triazole), 3,057 (C–H str., aromatic), 1,732 (C═O str. amide), 1,666 (N–H bending), 1,558, 1,502, and 1,442 (C═C str., aromatic) cm^{-1}. HRMS (ESI): *m/z* calculated for $[M+H]^+$ $C_{23}H_{20}N_6SO$ 429.1498; found 429.1496.

4.2 | Pharmacological assays

4.2.1 | α-Amylase inhibition assay

The activity was measured according to the published protocol with slight modifications.[39] The growing material was prepared by dissolving soluble starch (1 g) in 50 ml of 0.4 M NaOH and then heating it at 100°C for 5 min. The solution was cooled on crushed ice, and the pH of the solution was settled at 7 with 2 M HCl. Distilled water was added to make volume to 200 ml. A sample solution was prepared in DMSO with different concentrations, that is, 100, 50, 25, and 12.5 μg/ml. The growing material (20 μl) and sample solutions (10 μl) were added in a microplate well and the mixtures were incubated for 3 min at 37°C. Then, 10 μl of α-amylase solution (50 μg/ml) was added and the mixture was further incubated for 15 min at 37°C. The reaction was stopped by adding 40 μl of 0.1 M HCl and then 100 μl of 1 mM

iodine solution. The absorbances were recorded at 650 nm. Acarbose was used as a standard drug. α-Amylase activity was expressed in % inhibition.

$$\% \text{ Inhibition} = [1 - (Ab_1 - Ab_2)/(Ab_3 - Ab_4) \times 100],$$

where Ab_1 was the absorbance of solution holding starch and tested compounds, Ab_2 was the absorbance of solution holding amylase, starch and tested compound, Ab_3 was the absorbance of solution holding starch, and Ab_4 was the absorbance of solution holding amylase and starch.

4.2.2 | α-Glucosidase inhibition assay

A modified version of the assay described by Xaio et al.[3] was followed. A sample solution with various concentrations, that is, 100, 50, 25, and 12.5 μg/ml, was prepared in DMSO. A volume of 10 μl of the sample solution was diluted with 120 μl of phosphate buffer (100 mM) of pH 6.9. Then, 20 μl of 0.5 U/ml α-glucosidase enzymes was added into each well and the plates were incubated at 37°C for 15 min. Thereafter, 20 μl of pNPG (4-nitrophenyl-α-D-glucopyranoside) in potassium phosphate buffer (5 mM) was added to it, and the reaction mixture was further incubated for 15 min at 37°C. The absorbance was measured at 405 nm. For positive control, acarbose was used and DMSO (10 μl) was used at the place of sample solution for negative control. The equation for calculating percentage inhibition is as follows:

$$\% \text{ Inhibition} = ([Abs_{control} - Abs_{sample}]/Abs_{control}) \times 100,$$

where $Abs_{control}$ is the absorbance of the control and Abs_{sample} is the absorbance of the sample.

4.3 | Molecular docking

Homology modeling was performed for the determination of the three-dimensional structure of *Saccharomyces cerevisiae* α-glucosidase enzyme. The primary amino acid sequence was taken from Uniprot database (Universal Protein Resource) in FASTA format, with accession ID P53341. Homology modeling was done with SWISS-MODEL Homology Modeling web server.[40] The template for the protein sequence was searched with BLAST[41] and HHBlits,[42] and the crystal structure of oligo-1,6-glucosidase (3axh.1.A) with sequence identity 72.51% was chosen as a template for alignment of a target protein using ProMod3.[43] QMEAN scoring function[44] was used for assessing the global as well as per residue quality of the built model. The value of QMEAN was 0.04, which indicates a very good prediction of protein structure. MolProbity Ramachandran analysis[45] showed that 96.7% of all residues were in the favored region, whereas 100% residues were in the allowed region. This protein structure was used for docking studies and the protein active site was determined by identifying its binding residues as reported in literature.[46]

Compounds **4e**, **4g**, and **4n** were docked in this active site using AutoDock Vina.[47] The dimensions of the search box were as follows: center_*x* = −12.5327806063, center_*y* = −5.97621363233, center_*z* = −19.8977436728, size_*x* = 26.1196805853, size_*y* = 25.0, and size_*z* = 25.0. The results were analyzed using a Discovery Studio visualizer[48] and PyMOL.[49]

ACKNOWLEDGMENTS

Authors are highly thankful to DST-PURSE ([SR/PURSE Phase 2/40[G]), New Delhi, and Dr. APJ Abdul Kalam CIL, GJUS&T, Hisar. Mrs. Laxmi Deswal (SRF) acknowledges the University Grant Commission, New Delhi, India, for the award of JRF–SRF Fellowship with Sr. No. 2121410071, Ref. No. 21/12/2014(ii) EU-V, for financial assistance.

CONFLICT OF INTERESTS

The authors declare that there are no conflicts of interests.

ORCID

Vikas Verma http://orcid.org/0000-0002-6648-1877
Chander P. Kaushik http://orcid.org/0000-0001-7917-1280
Ashwani Kumar http://orcid.org/0000-0002-8966-3569

REFERENCES

[1] P. Saeedi, I. Petersohn, P. Salpea, B. Malanda, S. Karuranga, N. Unwin, S. Colagiuri, L. Guariguata, A. A. Motala, K. Ogurtsova, J. E. Shaw, D. Bright, R. Williams; the IDF Diabetes Atlas Committee, *Diabetes Res. Clin. Pract.* **2019**, *157*, 107843.
[2] M. A. Ibrahim, N. A. Koorbanally, S. Islam, *Acta Pharm.* **2014**, *64*, 311.
[3] J. B. Xiao, P. Hogger, *Curr. Med. Chem.* **2015**, *22*, 23.
[4] C. M. Ma, M. Hattori, M. Daneshtalab, L. Wang, *J. Med. Chem.* **2008**, *51*, 6188.
[5] L. Zeng, G. Zhang, Y. Liao, D. Gong, *Food Funct.* **2016**, *7*, 3953.
[6] W. Puls, H. P. Krause, L. Muller, H. Schutt, R. Sitt, G. Thomas, *Int. J. Obes.* **1984**, *8*, 181.
[7] N. K. N. Zawawi, M. Taha, N. Ahmat, A. Wadood, N. H. Ismail, F. Rahim, S. S. Azam, N. Abdullah, *Bioorg. Chem.* **2016**, *64*, 29.
[8] Y. E. Bakri, E. H. Anouar, I. Marmouzi, K. Sayah, Y. Ramli, M. E. A. Faouzi, E. M. Essassi, J. T. Mague, *J. Mol. Model.* **2018**, *24*, 179.
[9] R. Abraham, P. Periakaruppan, K. Mahendran, M. Ramanathan, *Microb. Pathog.* **2018**, *114*, 409.
[10] J. E. Cheong, M. Zaffagni, I. Chung, Y. Xu, Y. Wang, F. E. Jernigan, B. R. Zetter, L. Sun, *Eur. J. Med. Chem.* **2018**, *144*, 372.
[11] H. W. Ding, L. Yu, M. X. Bai, X. C. Qin, M. T. Song, Q. C. Zhao, *Bioorg. Chem.* **2019**, *93*, 103283.
[12] T. Pan, X. He, B. Chen, H. Chen, G. Geng, H. Luo, H. Zhang, C. Bai, *Eur. J. Med. Chem.* **2015**, *95*, 500.
[13] S. Yadav, B. Narasimhan, S. M. Lim, K. Ramasamy, M. Vasudevan, S. A. A. Shah, A. Mathur, *Egypt. J. Basic Appl. Sci.* **2018**, *5*, 100.
[14] R. Muluk, P. Kothawade, G. Kulkarni, P. Ingale, *World J. Pharm. Pharm. Sci.* **2018**, *7*, 1263.
[15] H. B. Liu, W. W. Gao, V. K. R. Tangadanchu, C. H. Zhou, R. X. Geng, *Eur. J. Med. Chem.* **2018**, *143*, 66.
[16] B. G. Youssif, Y. A. Mohamed, M. T. Salim, F. Inagaki, C. Mukai, H. H. Abdu-allah, *Acta Pharm.* **2016**, *66*, 219.
[17] F. Mir, S. Shafi, M. S. Zaman, N. P. Kalia, V. S. Rajput, C. Mulakayala, N. Mulakayala, I. A. Khan, M. S. Alam, *Eur. J. Med. Chem.* **2014**, *76*, 274.
[18] S. K. Avulaa, A. Khana, N. U. Rehmana, M. U. Anwara, Z. Al-Abria, A. Wadoodb, M. Riazb, R. Csukc, A. A. Harrasi, *Bioorg. Chem.* **2018**, *81*, 98.

[19] B. Madhavilatha, D. Bhattacharjee, G. Sabitha, B. V. S. Reddy, J. S. Yadav, N. Jain, B. J. M. Reddye, *J. Heterocycl. Chem.* **2018**, *55*, 863.
[20] A. A. Rashad, K. Acharya, A. Haft, R. Aneja, A. Dick, A. P. Holmes, I. Chaiken, *Org. Biomol. Chem.* **2017**, *15*, 7770.
[21] A. K. Kumar, V. Sunitha, B. Shankar, M. Ramesh, T. M. Krishna, P. Jalapathi, *Russ. J. Gen. Chem.* **2016**, *86*, 1154.
[22] K. T. Petrova, T. M. Potewar, P. C. Silva, M. T. Barros, R. C. Calhelha, A. Ciric, M. Sokovic, I. C. F. R. Ferreira, *Carbohydr. Res.* **2015**, *417*, 66.
[23] C. P. Kaushik, K. Kumar, K. Lal, B. Narasimhan, A. Kumar, *Monatsh.Chem.* **2016**, *147*, 817.
[24] Z. C. Daia, Y. F. Chena, M. Zhange, S. K. Lia, T. T. Yanga, L. Shenc, J. X. Wanga, S. S. Qiand, H. L. Zhud, Y. H. Ye, *Org. Biomol. Chem.* **2015**, *13*, 477.
[25] H. J. Kwak, Y. M. Pyun, J. Y. Kim, H. S. Pagire, K. Y. Kim, K. R. Kim, S. D. Rhee, W. H. Jung, J. S. Song, M. A. Bae, D. H. Lee, J. H. Ahn, *Bioorg. Med. Chem. Lett.* **2013**, *23*, 4713.
[26] M. Taha, N. H. Ismail, S. Imran, M. H. Mohamad, K. M. Khan, *Bioorg. Chem.* **2016**, *65*, 100.
[27] A. A. Adegboye, K. M. Khan, U. Salar, S. A. Aboaba, Kanwal, S. Chigurupati, I. Fatima, M. Taha, A. Wadood, J. I. Mohammad, H. Khan, *Eur. J. Med. Chem.* **2018**, *150*, 248.
[28] C. Gill, G. Jadhav, M. Shaikh, R. Kale, A. Ghawalkar, D. Nagargoje, M. Shiradkar, *Bioorg. Med. Chem. Lett.* **2008**, *18*, 6244.
[29] G. Wang, Z. Peng, J. Wang, J. Li, X. Li, *Bioorg. Med. Chem. Lett.* **2016**, *26*, 5719.
[30] G. J. Ye, T. Lan, Z. X. Huang, X. N. Cheng, C. Y. Cai, S. M. Ding, M. L. Xie, B. Wang, *Eur. J. Med. Chem.* **2019**, *177*, 362.
[31] B. J. Henderson, D. J. Carper, T. F. Gonzalez-Cestari, B. Yi, K. Mahasenan, R. E. Pavlovicz, M. L. Dalefield, R. S. Coleman, C. Li, D. B. McKay, *J. Med. Chem.* **2011**, *54*, 8681.
[32] C. A. Lipinski, F. Lombardo, B. W. Dominy, P. Feeney, *J. Adv. Drug Deliv. Rev.* **1997**, *23*, 4.
[33] D. F. Veber, S. R. Johnson, H. Y. Cheng, B. R. Smith, K. W. Ward, K. D. Kopple, *J. Med. Chem.* **2002**, *45*, 2615.
[34] S. Saini, D. Neerupma, A. Mittal, G. Kumar, *J. Drug Deliv. Ther.* **2016**, *6*, 100.
[35] M. R. Ahamed, S. F. Narren, A. S. Sadiq, *Al-Nahrain J. Sci.* **2013**, *16*, 77.
[36] M. N. S. Rad, S. Behrouz, M. M. Doroodmand, A. Movahediyan, *Tetrahedron* **2012**, *68*, 7812.
[37] M. N. S. Rad, S. Behrouz, S. J. Hoseini, H. Nasrabadi, M. S. Zare, *Helv. Chim. Acta* **2015**, *98*, 1210.
[38] M. N. S. Rad, Z. Asrari, S. Behrouz, G. H. Hakimelahi, A. Khalafi-Nezhad, *Helv. Chim. Acta* **2011**, *94*, 2194.
[39] Z. Xiao, R. Storms, A. Tsang, *Anal. Biochem.* **2006**, *351*, 146.
[40] A. Waterhouse, M. Bertoni, S. Bienert, G. Studer, G. Tauriello, R. Gumienny, F. T. Heer, T. A. P. Beer, C. Rempfer, L. Bordoli, R. Lepore, T. Schwede, *Nucleic Acids Res.* **2018**, *46*, W296.
[41] C. Camacho, G. Coulouris, V. Avagyan, N. Papadopoulos, J. Ma, K. Bealer, T. L. Madden, *BMC Bioinform.* **2009**, *10*, 421.
[42] M. Remmert, A. Biegert, A. Hauser, J. Soding, *Nat. Methods* **2012**, *9*, 173.
[43] N. Guex, M. C. Peitsch, T. Schwede, *Electrophoresis* **2009**, *30*, S162.
[44] P. Benkert, M. Biasini, T. Schwede, *Bioinformatics* **2011**, *27*, 343.
[45] L. W. Davis, A. Leaver-Fay, V. B. Chen, J. N. Block, G. J. Kapral, X. Wang, L. W. Murray, W. B. Arendall, J. Snoeyink, J. S. Richardson, D. C. Richardson, *Nucleic Acids Res.* **2007**, *35*, W375.
[46] G. Wang, Y. Peng, Z. Xie, J. Wang, M. Chen, *Med. Chem. Commun.* **2017**, *8*, 1477.
[47] O. Trott, A. J. Olson, *J. Comput. Chem.* **2010**, *31*, 455.
[48] Dassault Systemes Blovia Corp., *Discovery Studio Visualizer v17.2.0.16349*, San Diego, CA **2016**.
[49] Schrodinger, Inc., *Version 1.7.2.1., Open Source PyMOL(TM) Molecular Graphics System*, New York **2009-2014**.

SUPPORTING INFORMATION

Additional supporting information may be found online in the Supporting Information section.

How to cite this article: Deswal L, Verma V, Kumar D, et al. Synthesis and antidiabetic evaluation of benzimidazole-tethered 1,2,3-triazoles. *Arch Pharm.* 2020;e2000090.
https://doi.org/10.1002/ardp.202000090